



**Joint ICTP-IAEA Workshop on Simulation of Nuclear Reaction Data with the TALYS Code |
(SMR 3887)**

16 Oct 2023 - 20 Oct 2023
ICTP, Trieste, Italy

T01 - ALHASSAN Erwin

Bayesian model selection in TENDL-based evaluation of nuclear data

T02 - AYLLON UNZUETA Mauricio

Precision measurements of nuclear data for planetary nuclear spectroscopy

T03 - BASAK Dipali

Investigation of $^{113}\text{In}(\alpha, n)$ and $^{\text{nat}}\text{In}(\alpha, n)$ reactions to determine the alpha-optical potential for astrophysical p-process

T04 - BURAHMAH Naser

Cross-Section Measurement of Protactinium Isotopes Production Using Thorium-229

T05 - CANNAROZZO Simone

Global comparison between experimentally measured isomeric yield ratios and nuclear model calculations

T06 - CANTON Luciano

Applications of Nuclear-Reaction Theory in Medical Radionuclides Production.

T07 - DAHIYA Monika

Measurements of Nuclear reaction cross section on ^{68}Zn with complete uncertainty propagation and covariance analysis

T08 - DOROSTKAR Mokhtari Mahdieh

Excellent choice for investigating practical radioisotope production

T09 - FARZANEHPOOR ALWARS Ali

Neutron inelastic cross-section measurement at the GAINS spectrometer

T10 - GANDHI Aman

Cross section measurement for neutron-induced reaction

T11 - HARKI Glara Fuad Hasan

This work presents the evaluated results of cross-sections for natural chromium ($^{\text{nat}}\text{Cr}$) with several nuclear reactions of $^{\text{nat}}\text{Cr}(d, x)^{52}\text{g}$, $m\text{-Mn}$, $^{\text{nat}}\text{Cr}(d, x)^{54}\text{Mn}$, $^{\text{nat}}\text{Cr}(d, x)^{51}\text{Cr}$, and $^{\text{nat}}\text{Cr}(d, x)^{48}\text{V}$ using the statistical nuclear model EMPIRE 3.2.2 code with different level density models, for some radionuclides used in positron emission tomography. We compared the results to

T12 - HEHR Douglas Brian

Evaluation of Atomic Recoil Spectra for Studies of Degradation in Semiconductor Devices

T13 - HUSSAIN Mazhar

The use of TENDL global parameters and TALYS calculations for medical isotope production

T14 - KNIJPSTRA Jisk Klaas

Time-of-flight neutron elastic and inelastic cross section measurements with the ELISA neutron spectrometer

T15 - KUNITOMO Risa

Development of a detection technique of nuclear fuel materials using photonuclear reactions

T16 - LAPLACE Andre Thibault

Neutron inelastic scattering cross section measurements at Lawrence Berkeley National Laboratory

T17 - LASHKO Yuliia

^{47}Sc production for medical applications: cross-section optimization based on genetic algorithm

T18 - MARTÍN YI Jorge

Device and method for low-uncertainty and high-efficiency neutron time-of-flight spectrometry

T19 - MYAGMARJAV Odsuren

A Mirror $1/2^+$ states of ^{9}Be and ^{9}B in the complex scaling method

T20 - NGUYEN Bich Thuy

Thermal neutron capture cross-section and resonance integral measurements of $^{186}\text{W}(n,g)^{187}\text{W}$ reaction using the thermal column neutron source at the Dalat research reactor

T21 - PARVU Mihaela

Cross section uncertainties and their impact on background studies

T22 - SALINO Vivian

Nuclear data uncertainties and adjustments using deterministic and Monte-Carlo methods along with PWR measurements

T23 - SMOLOVIC Rade

Analysis of $^{209}\text{Bi}(g,xn)$ nuclear reactions

T24 - TATARI VARNOUSFADERANI Mansoureh

A theoretical study for the production of ^{32}P radioisotope using neutrons from the $^{68}\text{Zn}(p,n)^{68}\text{Ga}$ reaction in a medical cyclotron

T25 - TIMCHENKO S. Iryna

Cross-sections of photonuclear reactions $^{nat}\text{Ni}(\gamma,pxn)^{55-58}\text{Co}$: experimental and calculated in the TALYS code

T26 - TWISHA Munmun

Statistical Model Calculations with TALYS for Sn Isotopes

T27 - YETTOU Leila

Effects of level density a -parameter in the framework of preequilibrium model for $^{58}\text{Ni}(n, xp)$ reaction at 8, 9, 9.4 and 11 MeV

Bayesian model selection in TENDL-based evaluation of nuclear data

E. Alhassan¹, D. Rochman² and A.J. Koning^{3,4}

¹*(Presenting author underlined) Belgian Nuclear Research Centre (SCK CEN), Mol, Belgium*

²*Paul Scherrer Institute, Villigen, Switzerland*

³*International Atomic Energy Commission (IAEA), Vienna, Austria*

⁴*Uppsala University, Uppsala, Sweden*

If we assume that there exists one true model among a number of candidate nuclear reaction models used for nuclear data evaluation, we can select the 'best' model set, that is, the model combination closest to the true model set, using a number of Bayesian model selection criteria within a TENDL-based evaluation [1] framework. The selection methods considered in this work are the: (1) Bayes factor, (2) maximum likelihood estimation using Bayesian Monte Carlo and Backward Forward Monte Carlo weights, (3) Akaike Information Criterion (AIC) and, (4) Bayesian Information Criterion (BIC). Once the 'best' model set is determined, covariance information is subsequently obtained by varying parameters around this model combination. The method begins with the variation of many nuclear reaction models as well as their parameters as carried out in Refs. [2,3,4]. The random cross sections obtained were then compared with experimental data from the EXFOR database [5] using the selection criteria listed and applied to the evaluation of proton induced reactions on Ni-58 in the fast energy range below 100 MeV.

[1] A.J. Koning, D. Rochman, J-Ch. Sublet, N. Dzysiuk, M. Fleming, S. Van der Marck, Nuclear Data Sheets 155, 1-55 (2019).

[2] E Alhassan, D Rochman, A Vasiliev, M Hursin, AJ Koning, H Ferroukhi, Nuclear Science and Techniques 33 (4), 50(2022).

[3] E. Alhassan, D. Rochman, A. Vasiliev, R.M. Bergmann, M. Wohlmuther, A.J. Koning and H. Ferroukhi, EPJ Nuclear Sci. Technol. 8, 3 (2022).

[4] D. Rochman, A. Koning; S. Goriely, EPJ Web of Conferences 281, 00005 (2023).

[5] H. Henriksson, O. Schwerer, D. Rochman, M.V. Mikhaylyukova and N. Otuka, ND2007, 781-784 (2007).

Joint ICTP-IAEA Workshop on Simulation of Nuclear Reaction Data with the TALYS Code | (smr 3887)

Mauricio Ayllon Unzueta^{1,2}, Ann Parsons¹, Patrick Peplowski³, Arun Persaud⁴, and Jack Wilson³

¹ NASA Goddard Space Flight Center (USA)

² Catholic University of America (USA)

³ Johns Hopkins University Applied Physics Laboratory (USA)

⁴ Lawrence Berkeley National Laboratory (USA)

Neutron-induced gamma ray reactions including both inelastic scattering ($n, n'\gamma$) and radiative capture (n, γ) are important in several applications of applied nuclear physics that require non-destructive elemental assays of unknown materials. An example application is the Dragonfly Gamma ray and Neutron Spectrometer (DraGNS) onboard the NASA New Frontiers mission Dragonfly [1] that will explore Saturn's largest moon, Titan (Figure 1). Interpreting these gamma ray measurements requires precise knowledge of the energy and angle dependent reaction probabilities (cross sections, σ). However, there are large gaps and inconsistencies in public databases for several common elements that are relevant for most applications. These shortcomings can be addressed through a focused effort to benchmark nuclear data libraries and models with experimental datasets to identify and ultimately fix underlying library and model deficiencies. Specifically, we decided to focus on measuring inelastic scattering reactions at 14 MeV incident neutron energy in support of DraGNS and because of the wide use of Deuterium-Tritium (DT) sources in other fields. In this talk, I will present a proof-of-concept technique that we developed to measure ($n, n'\gamma$) cross sections with an Associated Particle Imaging (API) system, which allows a significant reduction in systematic uncertainties via accurate neutron flux measurements. I will further discuss how TALYS is used to design the experiment and how well its predicted cross section matches the results of our experiments. I will end by highlighting how we would like to improve our TALYS simulations to include angular dependence and other theoretical models.

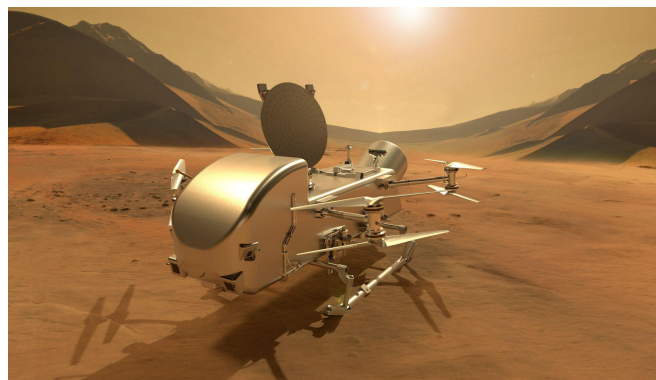


Figure 1: NASA mission Dragonfly will carry a DT neutron generator and a High-Purity Germanium (HPGe) detector to measure the surface elemental composition of Titan.

[1] Lorenz, R.D, Turtle, E.P, et al., "Dragonfly: A rotorcraft lander concept for scientific exploration at Titan," Johns Hopkins APL Technical Digest, 34(3), p.14 (2018).

Investigation of $^{113}\text{In}(\alpha, n)$ and $^{nat}\text{In}(\alpha, n)$ reactions to determine the α -optical potential for astrophysical p-process

Dipali Basak^{1,3}, Tanmoy Bar^{1,3}, Lalit Kumar Sahoo^{1,3}, Sukhendu Saha^{1,3}, Jagannath Datta², Sandipan Dasgupta², and Chinmay Basu¹

¹*Nuclear Physics Division, Saha Institute of Nuclear Physics, HBNI, I/AF, Bidhannagar, Kolkata-700064, India*

²*Analytical Chemistry Division, BARC unit, Variable Energy Cyclotron Centre, I/AF Bidhan Nagar, Kolkata-700064, India*

³*Homi Bhabha National Institute, Anushaktinagar, Mumbai, Maharashtra-400094, India*

The majority of heavy nuclei are synthesized in stars by neutron capture and β -decays in the s- or r-process. However, 30-35 neutron deficient nuclei (^{74}Se - ^{196}Hg), often called p-nuclei, are produced via photo-disintegration rather than neutron capture. In photo disintegration process, p-nuclei are formed by the (γ, n) , (γ, α) or (γ, p) reactions from s or r-seed nuclei in a high γ -flux scenario [1, 2]. The seed nuclei are initially moved towards the proton-rich side via a series of (γ, n) reactions. The (γ, p) and (γ, α) reactions are more rapid and produced stable elements with lower atomic number, when the neutron separation energy increases. It has been found that (γ, p) reactions are crucial for the formation of lower mass p-nuclei, whereas (γ, α) reactions produce medium and heavy masses. In comparison to s or r nuclei, p-nuclei are in general 10-100 times less abundant. However, the abundance of some p-nuclei is significantly higher. ^{113}In is a high abundant odd A p-nuclei (4.28%). Therefore, it is crucial to measure the ^{113}In production process more precisely to understand the discrepancy. The α -optical potential is one of the key input parameters used to measure the reaction rate of the (γ, α) -process using the Hauser-Feshbach(HF) statistical model and principle of detailed balance. The elastic scattering angular distribution data at high energies is used for determining the optical potential. Thus, a modification in potential is necessary for low energy astrophysical reactions. The (α, n) reaction, which is solely dependent on the α -transmission coefficient, i.e. on the alpha optical potential, is used to derive an alpha optical potential suitable for low energy reaction. In this work, $^{113}\text{In}(\alpha, n)$ and $^{nat}\text{In}(\alpha, n)$ reaction cross-sections were measured at K-130 cyclotron, VECC, Kolkata, using the activation method in the laboratory energy range 10-18 MeV. The measured (α, n) cross-sections data were analyzed in the framework of statistical model codes TALYS-1.96 [3] and obtained an energy dependent α -optical potential relevant for low energy astrophysical reactions.

[1] M. Arnould, S. Goriely, Phys. Rep. **384**, 184 (2003).

[2] S.E. Woosley, W.M. Howard, ApJS **36**, 285 (1978).

[3] A.J. Koning, S. Hilaire, S. Goriely, TALYS 1.96 A nuclear reaction program (2021).

Cross-Section Measurement of Protactinium Isotopes Production Using Thorium-229

Naser Burahmah¹, Justin Griswold², Lawrence Heilbronn³, Andrew Voyles⁴, and Lee Bernstein⁴

¹*Kuwait Foundation for the Advancement of Sciences, Kuwait*

²*Radioisotope Science and Technology Division, Oak Ridge National Laboratory, Oak Ridge, TN, USA*

³*Department of Nuclear Engineering, University of Tennessee, Knoxville, TN,, USA*

⁴*Nuclear Science Division, Lawrence Berkeley National Laboratory, Berkeley, CA 94720*

In this work, the previously unmeasured $^{232}\text{Th}(d,5n)^{229}\text{Pa}$ reaction is reported at deuteron energies of 31.0, 35.2, 41.4, and 49.6 MeV. The irradiation took place at the Lawrence Berkeley National Laboratory 88-Inch Cyclotron. The target processing and analysis were performed at Oak Ridge National Laboratory. The experiment used four thin foils ($\approx 17 \text{ mg/cm}^2$) of natural thorium metal in a stacked-target configuration, which were irradiated with a deuteron beam ($1 \mu\text{A}$) for approximately 11 continuous hours. Column chromatography techniques were implemented to directly assay ^{229}Pa and its low intensity γ -ray emissions. The measured peak of the excitation function of $^{232}\text{Th}(d,5n)^{229}\text{Pa}$ is $121.9 \pm 12.7 \text{ mb}$ at $E_d = 35.2 \text{ MeV}$. In addition to ^{229}Pa , the production cross sections of the $^{232}\text{Th}(d,xn)^{234-x}\text{Pa}$ reactions, where $x = 1, 2, 4,$ and 6 , are also reported and compared to previous measurements. The experimental cross sections were compared with calculated cross sections using several reaction modeling codes including PHITS, and TALYS as well as the evaluated nuclear reaction database TENDL.

Global comparison between experimentally measured isomeric yield ratios and nuclear model calculations

Simone Cananrosso¹, S. Pomp¹, A. Koning², A. Al-Adili¹, A. Göök¹ and A. Solders¹

¹*Uppsala University*

²*IAEA*

The level density steers transition probabilities between different states in the decay and de-excitation of excited nuclei. Reliable level density modelling is, therefore, key in describing, e.g., de-excitation of fission fragments, with implications on neutron and gamma multiplicities, and also manifested in the population of isomeric states.

We test six currently used level density models and the spin distribution in the level density by comparing calculations with measured isomeric yield ratios. The model calculations are performed with the TALYS code and experimental data for nuclear reactions populating spin isomers are retrieved from the EXFOR database.

On average, calculations are in agreement with measured data. However, we find that the population of the high-spin state in an isomeric pair is clearly favoured in all of the six studied level density models. Further studies are then performed on the three used phenomenological level density models. We find that a global reduction of the spin width distribution in these models by about a factor of two would remedy this problem and improve the agreement between calculated and experimentally observed isomeric yield ratios. This result is independent of the incident particle in the nuclear reaction.

The needed reduction of the spin width distribution to comply with empirical data has, e.g., implications for studies in angular momentum generation in fission using isomeric yield ratios[1], calculations of anti-neutrino spectra from nuclear reactors, as well as neutron and gamma-ray multiplicities in nuclear reactor calculations[2].

This work led to a manuscript that is currently under review.

- [1] Rakopoulos, V. and Lantz, M. and Solders, A. and Al-Adili, A. and Mattera, A. and Canete, L. and Eronen, T. and Gorelov, D. and Jokinen, A. and Kankainen, A. and Kolhinen, V. S. and Moore, I. D. and Nesterenko, D. A. and Penttilä, H. and Pohjalainen, I. and Rinta-Antila, S. and Simutkin, V. and Vilén, M. and Voss, A. and Pomp, S., *Physical Review C* **98**, 2, (2018).
- [2] Piau, V. and Litaize, O. and Chebboubi, A. and Oberstedt, S. and Göök, A. and Oberstedt, A., *Physics Letters, Section B: Nuclear, Elementary Particle and High-Energy Physics* **837** (2023).

Applications of Nuclear-Reaction Theory in Medical Radionuclides Production

L.Canton¹, Y. Lashko¹, F. Barbaro¹, and L. Zangrando¹

¹*INFN Sezione di Padova, Italy*

In collaboration with INFN-LNL (Laboratori Nazionali di Legnaro), we have simulated various nuclear reactions of interest for the cyclotron production of innovative radionuclides for targeted therapies and nuclear-medicine diagnostics. Interdisciplinary LNL projects such as PASTA, REMIX, METRICS, CUPRUM-TTD, and SPES_MED have been carried out or have been started to assess the feasibility for the production of innovative radionuclides for teragnostic applications (⁴⁷Sc, ⁶⁷Cu, etc.) or for innovative imaging (¹⁵⁵Tb, ^{52g}Mn, etc.). An overview of the importance of nuclear-reaction simulations will be illustrated with specific examples on how TALYS can be employed in this applied research field [1].

[1] A. Colombi, M. P. Carante, F. Barbaro, L. Canton, A. Fontana, Nuclear Technology, **208**, 735 (2022).

Neutron Capture Cross Section on ^{68}Zn with complete uncertainty propagation and covariance analysis

Monika¹, * A. Gandhi¹, S. Lawitlang², Sumit¹, B. Lalremruata^{2,5}, A. Kumar¹, Rajeev Kumar^{3,5}, L. S. Danu⁴, S. Santra^{4,5}, B. K. Nayak⁵, and Rebecca Pachua¹

¹Department of Physics, Banaras Hindu University, Varanasi-221005, INDIA

²Department of Physics, Mizoram University, Tanhril, Aizawl-796004, INDIA

³Reactor Physics Design Division, Bhabha Atomic Research Center, Mumbai-400085, INDIA

⁴Nuclear Physics Division, Bhabha Atomic Research Centre, Mumbai-400085, INDIA and

⁵Homi Bhabha National Institute, Anushaktinagar, Mumbai-400094, INDIA

1. Introduction

The neutron cross sections are useful especially in the design of fusion reactor, fission reactor and accelerator system. And the experimental data are useful in improving the accuracy and reliability of theoretical nuclear models and evaluated nuclear data libraries. Zinc is important in reactor to decrease the radiation knowledge of neutron induced fields and primary water stress corrosion cracking (Choi et al., 2019) [1]. ZnO crystal has damage-recoverable of high-flux-radiation and has been considered a potential window material for fusion reactor (Yamanoi et al., 2016) [2].

2. Experimental Details

The experiment was performed at Bhabha Atomic Research Centre (BARC), Mumbai and at the Folded Tandem Ion Accelerator (FOTIA) facility was used for the production of proton beam [3]. Proton with energies 2.50 ± 0.02 , 3.28 ± 0.02 , 2.70 ± 0.02 , 4.30 ± 0.02 , 3.50 ± 0.02 , 3.00 ± 0.02 , 5.00 ± 0.02 MeV were used for irradiation. Indium monitor was placed for every sample. The stack foil activation technique was used followed by off line gamma ray spectroscopy on HPGe detector.

3. Result

The measured values of $^{68}\text{Zn}(n,\gamma)^{69}\text{Zn}^m$ reaction cross section at neutron energies as well as their uncertainties and correlation coefficients. And the Cross-section values reported are compared with data available in literature, theoretical calculations using the Tallys-1.95 and the evaluated data from EXFOR [4] in fig.1 and fig.2. Detailed results will be discussed during the conference.

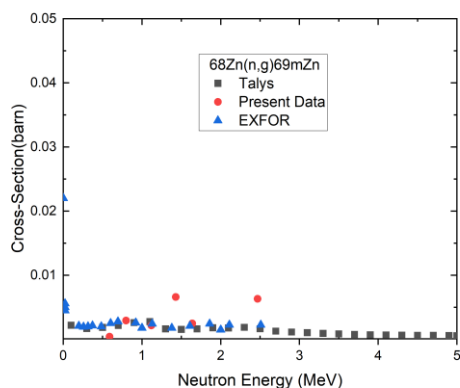


Fig.1

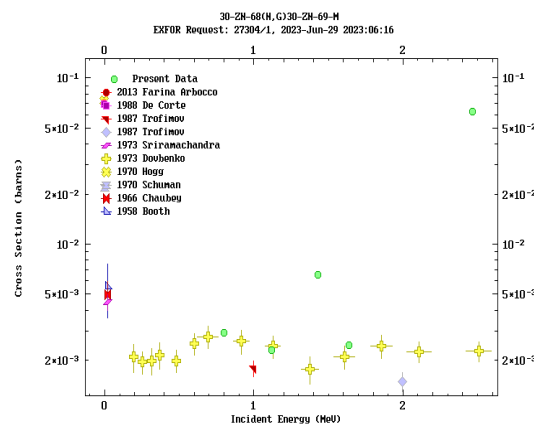


Fig.2

[1] Choi, J.S., Park, S.C., Park, K.R., Yang, H.Y., B., Y.O., 2013. Effect of zinc injection on the corrosion products in nuclear fuel assembly. Nat. Sci. 05, 173–181

[2] Yamanoi, K., Empizo, M.J.F., Mori, K., Iwano, K., Minami, Y., Arita, R., Iwasa, Y., Norimatsu, T., Hangyo, M., Azechi, H., Fukuda, T., Singidas, B.G., Sarmago, R.V., Oya, M., Ueda, Y., 2016. ZnO crystal as a potential damage-recoverable window material for fusion reactors. Opt. Mater. 62 646–650

[3] P. Singh et al., Physical Review C 14, 438 (1976)

[4] EXFOR database, <https://www-nds.iaea.org/exfor/exfor.html>

TALYS can be used as a great choice for investigating practical radioisotope production in both industry or medicine, radioisotopes like Ge-68, Cd-110 and etc. Selecting an appropriate radioisotope is an important step so that the chosen candidate either does not have long lasting half life so that it can't be used in short time projects or so short so that it can not be used in imaging as well as long therapies and etc. For example, $^{65}\text{Cu}(n,p)^{65}\text{Ni}$ is a common reaction for Ni production which is useful in nuclear medicine.

In addition, there are some nuclear models in TALYS that can be distinctly considered for cross section or production interest calculations. Models such as GSM, BSFGM, ... the accomplished work will be validated in the case of comparing the calculation with previous works or codes.

Neutron inelastic cross-section measurement at the GAINS spectrometer

A. Farzanehpoor Alwars, M. Kavatsyuk, N. Kalantar-Nayestanaki

Energy and Sustainability Research Institute Groningen, University of Groningen

The development of safer Generation IV reactors is a crucial step towards achieving the goals of clean, secure, and affordable electricity. In order to accomplish this, a comprehensive understanding of the neutron inelastic cross-sections of the various materials present within the reactor is essential. To obtain these valuable insights, neutron time of flight experiments are conducted, employing advanced techniques such as the utilization of the GAINS spectrometer at the GELINA facility[1].

The GELINA facility provides an electron linear accelerator (LINAC), which enables the generation of a wide-ranging neutron beam (thermal to 2 MeV) through the utilization of photoneutron and fission reactions. This neutron beam is then directed towards specific target materials, such as ^{14}N or ^{56}Fe , resulting in interactions between the neutrons and the targets. These interactions give rise to the emission of gamma-rays with known energies. By meticulously analyzing the resulting gamma-ray spectrum and taking into consideration the precise time of flight of the neutrons, it becomes possible to calculate the neutron cross-section [?]. The primary focus of our research lies in the measurement of the neutron inelastic cross-section, with the ultimate aim of utilizing the obtained data to enhance the existing models employed in reactor design and analysis.

To address the need for improved resolution of the High-Purity Germanium (HPGe) detectors utilized at the GAINS spectrometer and to overcome issues related to pulse pile-ups, a new fast digitizer has been implemented. This state-of-the-art digitizer boasts remarkable specifications, including a 14-bit resolution, operating at a frequency of 250 MHz, and featuring 16 channels. By employing the new digitizer, we aim to enhance the accuracy and reliability of data acquisition during neutron time of flight experiments, thus ensuring the integrity of the measurements. Furthermore, it should be emphasized that upon obtaining successful measurements and carefully considering all associated uncertainties, the resulting data can be effectively validated using the widely recognized TALYS code, contributing to the overall confidence and credibility of our findings.

[1] L. C. Mihailescu, C. Borcea, A. J. Koning, A. J. M. Plompen, Nucl. Phys. A. **786**, 1 (2007).

[2] A. Negret, L. C. Mihailescu, C. Borcea, Ph. Dessagne, K. H. Guber, M. Kerveno, A. J. Koning, A. Olacel, A. J. M. Plompen, C. Rouki and G. Rudolf, Phys. Rev. C **91**, 064618 (2015).

Cross section measurement for neutron-induced reaction

A. Gandhi¹

¹*Horia Hulubei National Institute of Physics and Nuclear Engineering - IFIN-HH, Bucharest, 077125, Romania*

In order to develop new applications and advanced technologies the worldwide scientific community requires very precise and highly reliable cross-section measurements. In this talk, I will present a measurement of neutron-induced (n, γ), (n,p), & (n,2n) reaction cross sections in the fast neutron energy region using FOTIA and PURNIMA facilities at BARC, India [1-2]. I will further talk about the work carried out at IFIN-HH related to preparation of a neutron capture cross-section measurement at the n_TOF facility at CERN [3].

References

1. A. Gandhi, Aman Sharma, A. Kumar, Rebecca Pachuau, B. Lalremruata, S.V. Suryanarayana, L.S. Danu, Tarun Patel, Saroj Bishnoi, B.K. Nayak, *European Physical Journal A*, 57, 1 (2021).
2. A. Gandhi, Aman Sharma, Rebecca Pachuau, B. Lalremruata, Mayur Mehta, Prashant N Patil, S.V. Suryanarayana, L.S. Danu, B.K. Nayak, A. Kumar, *Physical Review C*, 102, 014603 (2020).
3. <https://www.nipne.ro/proiecte/pn3/ntof/>

Glara Fuad Hasan^{1,2,3,*}, Edrees Muhammad-Tahir Nury¹, Flavia Groppi^{2,3}

¹ Department of Physics, College of Education, University of Salahaddin, Erbil, Iraq

² Department of Physics, University of Milan, Milan, Italy

³ Accelerator and Superconductivity Laboratory (LASA),
Department of Physics, University of Milan and the National Institute of Nuclear Physics (INFN),
Segrate (MI), Italy

*Corresponding author: gelara.hassan@su.edu.krd

EVALUATION OF CROSS-SECTION DATA FOR RADIONUCLIDES USED IN POSITRON EMISSION TOMOGRAPHY BY EFFECTS OF LEVEL DENSITY MODELS USING EMPIRE 3.2.2 CODE

This work presents the evaluated results of cross-sections for natural chromium (^{nat}Cr) with several nuclear reactions of $^{nat}\text{Cr}(d, x)^{52g, m+}\text{Mn}$, $^{nat}\text{Cr}(d, x)^{54}\text{Mn}$, $^{nat}\text{Cr}(d, x)^{51}\text{Cr}$, and $^{nat}\text{Cr}(d, x)^{48}\text{V}$ using the statistical nuclear model EMPIRE 3.2.2 code with different level density models, for some radionuclides used in positron emission tomography. We compared the results to data sets found in literature, and data chosen from various sets of the electronic TENDL library.

Keywords: Mn radioisotopes, positron emission tomography scan, cross-section, nuclear medicine, EMPIRE 3.2.2 code.

1. Introduction

The use of radioisotopes in nuclear medical imaging has grown through revolution and evolution, largely attributable to the development of a new nuclear imaging technology [1]. The positron emission tomography (PET) is defined as a nuclear medical imaging technique with the specificity and sensitivity necessary for imaging molecular pathways in a non-invasive, and in vivo manner [2, 3]. Given the growing interest in therapeutic and nuclear medicine imaging, the demand for more and different radionuclides has increased. Importantly, types of radionuclides play significant roles in new technological applications for use in daily life, as well as in scientific research [4 - 6]. The ^{52}Mn radionuclide has paramagnetic parameters and is potentially important in image development as a contrast agent for manganese-enhance magnetic resonance imaging (MEMRI) and magnetic resonance imaging (MRI). In addition, ^{52g}Mn can be used for dual PET/MRI. The best manganese to use in this case has a suitable half-life, such as ^{52}Mn (5.591 days), ^{52m}Mn (21.1 min), particularly for use as a PET tracer in PET imaging [7]. To optimize the production routes, the deuteron induced cross-section is desired, for the optimization of the radioisotope produced, full knowledge of the input parameter EMPIRE code to obtain cross-sections data can be used to test the various nuclear level density of the nuclear reaction. For some of the radioisotopes that were used to get the PET image, the deuteron cross-section induced by nuclear reactions was calculated aided an EMPIRE

3.2.2 code, the most updated version of the simulation series [8]. Therefore, these deuteron-induced cross-section data sets obtained from theoretical models play an important role in the study of deuteron-induced nuclear reactions and they can be used by evaluators to interpolation and extrapolation.

The evaluation of cross-sections for the deuteron energy up to 35 MeV has been done by using the EMPIRE 3.2.2 code contributing various density level models for the excitation functions of $^{52g, m+}\text{Mn}$, ^{54}Mn , ^{51}Cr , and ^{48}V . The obtained results were compared and analyzed with literature data as well as TENDL electronic library.

2. EMPIRE model calculations

Cross-section determination plays an important role in the development of the calculations of nuclear reaction models. This work is focused on the calculations that were carried out with the nuclear reaction simulation EMPIRE code. The EMPIRE 3.2.2 code (theoretical computer code of nuclear reactions) approach was developed by Herman et al. and is useful to estimate the evaluated nuclear cross-section data sets of various particles and a broad range of energies. In this computer code, each of the input parameters has a significant role in the results. An input parameter is based on the Reference Input Parameter Library or RIPL-3, a library covering nuclear masses, discrete levels, optical models, decay schemes, and the levels of densities parameters. The optical model parameters in the calculations were

obtained from RIPL-3, the optical model potential (OMP) of deuteron energy used was proposed by Haixia An and Chonghai Cai [9]. Since the OMP was selected for use in this study, the densities of the nuclear levels were provided by means of different parameters. The statistical calculation of various nuclear-level density parameters was employed to estimate the cross-sections. Considering this, we can see the different results of different level density models factor for other medical radioisotopes [10 - 15]. In EMPIRE 3.2.2 the results of the cross-section substantially depend on the parameters of the level density. Each model of nuclear level density is related to different parameterizations concerning considerations of deformation and the excitation energy and collective phenomena of the target nuclei. This present simulation included the following level density models.

LEV DEN = 0 is the EMPIRE enhanced generalized superfluid model (EGSM), designed to (RIPL-3) to separate the levels and experimental value of D_{obs} . This is a default model used in EMPIRE code.

LEV DEN = 1 is the EMPIRE generalized superfluid model (GSM), designed to RIPL to separate the levels and experimental value of D_{obs} .

LEV DEN = 2 is the EMPIRE Gilbert - Cameron model (GCM), designed to RIPL to separate the levels and experimental value of D_{obs} (it stimulates separating the excitation energy into two different parts; in each of the regions, different forms functional of level densities are used).

LEV DEN = 3 is the RIPL-3 microscopic Hartree - Fock - Bogoliubov model (HFBM), D_{obs} is the neutron resonance spacing [16].

The obtained results by default LEV DEN = 0 in EMPIRE 3.2.2 code for all four reactions were not in accord with our experimental data sets up to 35 MeV

[17], in this case for to have a suitable curve for the calculated simulation achievement results and the available experimental data sets, to adjust the value of the default level density in EGSM [18], in adjusting the asymptotic value of a-parameter, that is equivalent to fix the parameter of level density, to obtain good results for each reaction and comparison with the experimental data, both the ATILNO and GTILNO values were fixed at 1.3.

3. Results and discussion

We calculated the cross-sections of activation products induced by ${}^{\text{nat}}\text{Cr}(d, x){}^{52\text{g.m}+}\text{Mn}$, ${}^{\text{nat}}\text{Cr}(d, x){}^{54}\text{Mn}$, ${}^{\text{nat}}\text{Cr}(d, x){}^{51}\text{Cr}$ and ${}^{\text{nat}}\text{Cr}(d, x){}^{48}\text{V}$ for each of the reactions using a default model and another three different level-density models LEV DEN = 1, 2, and 3. We approached the cross-section changes with different value of LEV DEN. The results achieved by EMPIRE were calculated, compared, and evaluated with other literature data sets and data taken from various versions of the online electronic TENDL library 2010 [19], 2012 [20], 2013 [21], 2014 [22], 2015 [23], 2017 [24] and 2019 [25], as shown in Figs. 1 - 4.

3.1. ${}^{\text{nat}}\text{Cr}(d, x){}^{52\text{g.m}+}\text{Mn}$

The theoretical calculated results for the reaction of ${}^{\text{nat}}\text{Cr}(d, x){}^{52\text{g.m}+}\text{Mn}$ were obtained using the EMPIRE code (Fig. 1) with available data from Burgus et al. (1954) [26], Kafalas et al. (1956) [27], Cheng Xiaowu et al. (1966) [28], Cogneau et al. (1966) [29], West et al. (1987) [30], Hermanne et al. (2011) [31], Alherbi, (2016) [32], Šimečková et al. (2018) [33] and Bianchi et al. (2020) [17]. The calculation was done using all four level-density models for ${}^{\text{nat}}\text{Cr}(d, x){}^{52\text{g.m}+}\text{Mn}$ nuclear reaction.

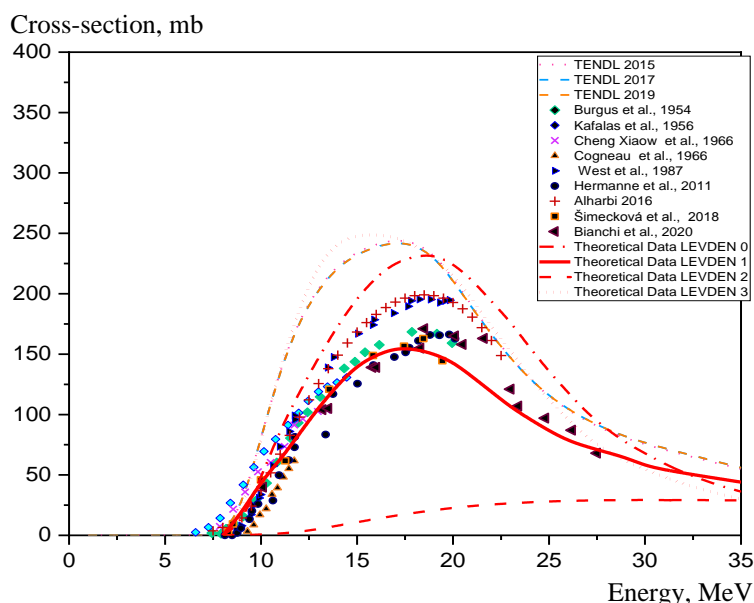


Fig. 1. Theoretical cross-section for ${}^{\text{nat}}\text{Cr}(d, x){}^{52\text{g.m}+}\text{Mn}$ by different nuclear level density models using EMPIRE 3.2.2 code. (See color Figure on the journal website.)

As shown in Fig. 1, the cross-section changed with each level-density model. In our experimental-group excitation-function data [17], we were able to calculate the contribution of the cross-section corresponding with the total decay of isomers in relation to the cumulative output of ^{52g}Mn [34]. Therefore, in this nuclear reaction, we also considered the theoretical data as experimental for the calculation of $^{52g,m+}\text{Mn}$.

It should be noted that our obtained EMPIRE results have a very good agreement, and the shape of the curve matched all the experimental data sets and TENDL. In the case where we select LEVDEN = 1, we clearly saw that other LEVDEN were significantly different from the experimental data sets. For LEVDEN = 0 the calculated results shown did not match but were higher than all experimental data sets. The LEVDEN = 2 model results predicted a much lower values compared to the results obtained in the

experimental cross-section. The LEVDEN = 3 results had good agreement with TENDL-2015, TENDL-2017, and TENDL-2019, and the curve was higher than in the other data sets.

3.2. $^{nat}\text{Cr}(d, x)^{54}\text{Mn}$

The theoretical EMPIRE 3.2.2 code results for the reaction $^{nat}\text{Cr}(d, x)^{54}\text{Mn}$ are shown in Fig. 2. In EMPIRE code, the data are clearly showing disagreement with each other, due to different level densities parameterization. The obtained results with the LEVDEN = 1 illustrate a good agreement with the literature and TENDL data sets. However, LEVDEN = 0 in the deuteron energy range 5 - 20 MeV shows a different shape of the curve; LEVDEN = 3 is giving good fitting only with data of Kafalas et al. (1956) [27], LEVDEN = 2 produces higher values in comparison with experimental data at above 20 MeV energies.

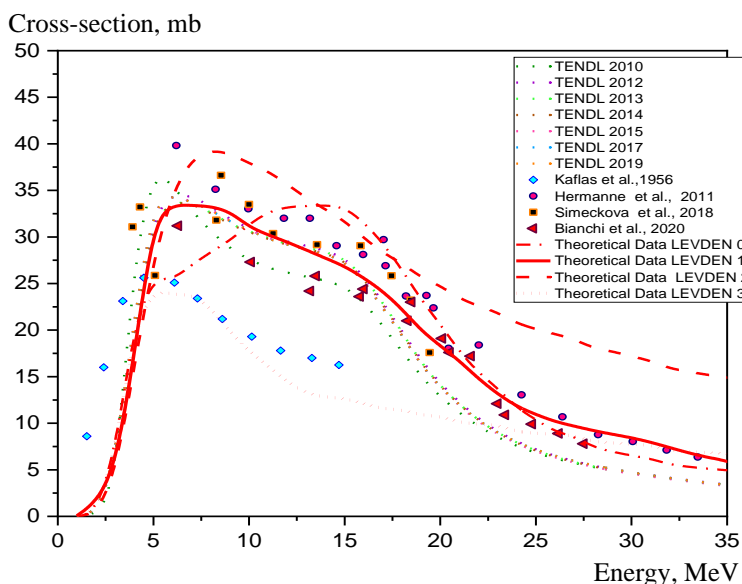


Fig. 2. Theoretical cross-section for $^{nat}\text{Cr}(d, x)^{54}\text{Mn}$ by different nuclear level density models using EMPIRE 3.2.2 code. (See color Figure on the journal website.)

3.3. $^{nat}\text{Cr}(d, x)^{51}\text{Cr}$

The theoretical calculations of the $^{nat}\text{Cr}(d, x)^{51}\text{Cr}$ for deuteron energy up to 35 MeV are shown in Fig. 3. The EMPIRE code results show that all level densities LEVDEN = 0, 1, and 3 are close to each other demonstrating good accordance with all experimental data. Furthermore, the results of LEVDEN = 1 show a perfect agreement with the results of Coetzee et al. (1972) up to 5.57 MeV [35], and as well as with both Klien et al. (2000) data sets giving good agreement up to 13.34 MeV [36]. In addition, in LEVDEN = 2 model the cross-section values do not reproduce the experimental data above 15 MeV and also the shape of the excitation curve has a dissimilar shape compared with other experimental and TENDL data sets.

3.4. $^{nat}\text{Cr}(d, x)^{48}\text{V}$

The theoretical calculations of the $^{nat}\text{Cr}(d, x)^{48}\text{V}$ reaction are shown in Fig. 4. The obtained results predicted by LEVDEN = 1 model are in accordance with all experimental and TENDL data sets. Moreover, the experimental data by Baron et al. (1963) [37] at energy 18.7 MeV show a good agreement with our results obtained with the GSM level-density model. The outcomes with LEVDEN = 0 and LEVDEN = 3 models are very close only at energies less than 25 MeV. Obtained results with LEVDEN = 2 model have shown an extremely high cross-section in respect to the experimental ones, the property of this level density model is due to the non-consideration of misshaping.

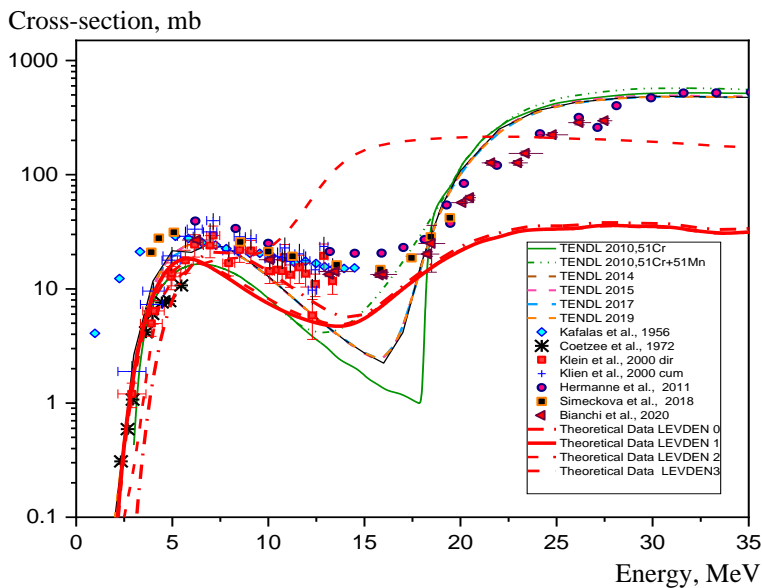


Fig. 3. Theoretical cross-section for ${}^{\text{nat}}\text{Cr}(d, x){}^{51}\text{Cr}$ by different nuclear level density models using EMPIRE 3.2.2 code. (See color Figure on the journal website.)

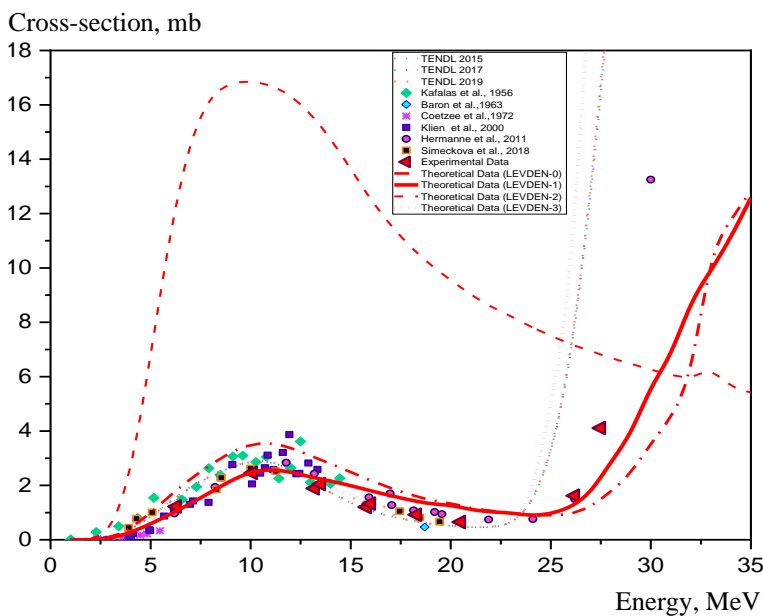


Fig. 4. Theoretical cross-section for ${}^{\text{nat}}\text{Cr}(d, x){}^{48}\text{V}$ by different nuclear level density models using EMPIRE 3.2.2 code. (See color Figure on the journal website.)

4. Conclusions

In this study, calculated theoretical cross-sections of ${}^{\text{nat}}\text{Cr}(d, x){}^{52\text{g.m}+}\text{Mn}$, ${}^{\text{nat}}\text{Cr}(d, x){}^{54}\text{Mn}$, ${}^{\text{nat}}\text{Cr}(d, x){}^{51}\text{Cr}$ and ${}^{\text{nat}}\text{Cr}(d, x){}^{48}\text{V}$ reactions were studied using the EMPIRE 3.2.2 computer code with various nuclear level-density models. In EMPIRE code, it is obtained that for all reactions ${}^{\text{nat}}\text{Cr}(d, x){}^{52\text{g.m}+}\text{Mn}$, ${}^{\text{nat}}\text{Cr}(d, x){}^{54}\text{Mn}$, ${}^{\text{nat}}\text{Cr}(d, x){}^{51}\text{Cr}$ and ${}^{\text{nat}}\text{Cr}(d, x){}^{48}\text{V}$, the estimated cross-section with parameter LEVDEN = 1 illustrated a good agreement with experimental data. Therefore, LEVDEN = 1 is the best option for the estimation and calculation.

The cross-sections data with LEVDEN = 2 did not show a radical agreement to that found in literature and experimental data. In addition, the predicted cross-section data for LEVDEN = 0 and LEVDEN = 3 is found suitable only for the small, limited range of

energy. These calculation results can be advantageous to develop the theoretical models, based on important phenomenological parameters.

We adjusted the input default parameter data for EMPIRE code for each of nuclear reactions ${}^{\text{nat}}\text{Cr}(d, x){}^{52\text{g.m}+}\text{Mn}$, ${}^{\text{nat}}\text{Cr}(d, x){}^{54}\text{Mn}$, ${}^{\text{nat}}\text{Cr}(d, x){}^{51}\text{Cr}$, and ${}^{\text{nat}}\text{Cr}(d, x){}^{48}\text{V}$, in order to achieve good agreement with the experimental data. We can conclude that our theoretical calculations are better than those given by the TALYS code. As a result, the theoretical predictions are very close to experimental data. For this reason, the theoretical description is recommended in cases when experimental measurements are difficult to perform.

The work was performed in the cooperation framework of the research Salahaddin University-Erbil and project METRICS by INFN (Italian National Institute of Nuclear Physics, CSN5). The cyclotron ARRONAX is supported by the European Union.

REFERENCES

1. N. Ramamoorthy. Impact of nuclear medicine and radiopharmaceuticals on health-care delivery: Advances, lessons, and need for an objective value-matrix. *Indian Journal of Nuclear Medicine* 33(4) (2018) 273.
2. *Beneficial Use and Production of Isotopes. 2000 Update* (Nuclear Energy Agency, OECD, 2000) 82 p.
3. L. Jødal, C. Le Loirec, C. Champion. Positron range in PET imaging: non-conventional isotopes. *Physics in Medicine & Biology* 59(23) (2014) 7419.
4. P. Martini. High-Yield Cyclotron Production of Metallic Radioisotopes for Nuclear Medicine. Ph.D. Thesis (Italy, Università degli Studi di Ferrara, 2017).
5. S. Jادیappa. Radioisotope: Applications, Effects, and Occupational Protection. In: *Principles and Applications in Nuclear Engineering - Radiation Effects, Thermal Hydraulics, Radionuclide Migration in the Environment*, 2018.
6. M.A. Synowiecki, L.R. Perk, J.F.W. Nijssen. Production of novel diagnostic radionuclides in small medical cyclotrons. *EJNMMI Radiopharmacy and Chemistry* 3 (2018) art. 3.
7. G. Saar et al. Anatomy, functionality, and neuronal connectivity with manganese radiotracers for positron emission tomography. *Molecular Imaging and Biology* 20(4) 2018 562.
8. M. Herman et al. EMPIRE: nuclear reaction model code system for data evaluation. *Nuclear Data Sheets* 108(12) (2007) 2655.
9. H. An, C. Cai. Global deuteron optical model potential for the energy range up to 183 MeV. *Phys. Rev. C* 73(5) (2006) 054605.
10. M. Şekerci, H. Özdoğan, A. Kaplan. Investigation on the Different Production Routes of Ga-67 Radioisotope by Using Different Level Density Models. *Moscow University Physics Bulletin* 74(3) (2019) 277.
11. M. Şekerci, H. Özdoğan, A. Kaplan. An investigation of effects of level density models and gamma ray strength functions on cross-section calculations for the production of ^{90}Y , ^{153}Sm , ^{169}Er , ^{177}Lu and ^{186}Re therapeutic radioisotopes via (n, γ) reactions. *Radiochimica Acta* 108(1) (2020) 11.
12. H. Özdoğan, M. Şekerci, A. Kaplan. Investigation of gamma strength functions and level density models effects on photon induced reaction cross-section calculations for the fusion structural materials $^{46,50}\text{Ti}$, ^{51}V , ^{58}Ni and ^{63}Cu . *Applied Radiation and Isotopes* 143 (2019) 6.
13. M. Şekerci, H. Özdoğan, A. Kaplan. Level density model effects on the production cross-section calculations of some medical isotopes via (α, xn) reactions where $x = 1 - 3$. *Modern Physics Letters A* 35(24) (2020) 2050202.
14. H. Özdoğan, M. Şekerci, A. Kaplan. An Investigation on the Effects of Some Theoretical Models in the Cross-Section Calculations of $^{50,52,53,54}\text{Cr}$ (α, x) Reactions. *Phys. Atom. Nucl.* 83(6) (2020) 820.
15. H. Özdoğan et al. Estimations of level density parameters by using artificial neural network for phenomenological level density models. *Applied Radiation and Isotopes* 169 (2021) 109583.
16. M. Herman et al. EMPIRE-3.2 Malta modular system for nuclear reaction calculations and nuclear data evaluation. User's Manual. INDC(NDS)-0603, BNL-101378-2013 (Brookhaven National Laboratory, National Nuclear Data Center, 2013) 297 p.
17. F. Bianchi et al. On the production of ^{52g}Mn by deuteron irradiation on natural chromium and its radionuclidic purity. *Applied Radiation and Isotopes* 166 (2020) 109329.
18. A. D'Arrigo et al. Semi-empirical determination of the shell correction temperature and spin dependence by means of nuclear fission. *Journal of Physics G: Nuclear and Particle Physics* 20(2) (1994) 365.
19. <https://www-nds.iaea.org/public/download-endf/TENDL-2010/>
20. <https://www-nds.iaea.org/public/download-endf/TENDL-2012/>; J. Koning, D. Rochman. Modern Nuclear Data Evaluation with the TALYS Code System. *Nuclear Data Sheets* 113(12) (2012) 2841.
21. <https://www-nds.iaea.org/public/download-endf/TENDL-2013/>
22. <https://www-nds.iaea.org/public/download-endf/TENDL-2014/>
23. https://tendl.web.psi.ch/tendl_2015/tendl2015.html
24. https://tendl.web.psi.ch/tendl_2017/reference.html; <https://www-nds.iaea.org/public/download-endf/TENDL-2017/>.
25. https://tendl.web.psi.ch/tendl_2019/talys.html; <https://www-nds.iaea.org/public/download-endf/TENDL-2019/>; J. Koning et al. TENDL: Complete Nuclear Data Library for Innovative Nuclear Science and Technology. *Nuclear Data Sheets* 155 (2019) 1.
26. W.H. Burgus et al. Cross Sections for the Reactions $\text{Ti}^{48}(\text{d}, 2\text{n})\text{V}^{48}$, $\text{Cr}^{52}(\text{d}, 2\text{n})\text{Mn}^{52}$; and $\text{Fe}^{56}(\text{d}, 2\text{n})\text{Co}^{56}$. *Phys. Rev.* 95(3) (1954) 750.
27. P. Kafalas, J.W. Irvine Jr. Nuclear excitation functions and thick target yields: $(\text{Cr} + \text{d})$. *Phys. Rev.* 104(3) (1956) 703.
28. C. Xiaowu et al. Some measurements of deuteron induced excitation function at 13 MeV. *Acta Physica Sinica* 22 (1966) 250.
29. M. Cogneau, L. Gilly, J. Cara. Absolute cross sections and excitation functions for deuteron-induced reactions on chromium between 2 and 12 MeV. *Nuclear Physics A* 99(1) (1967) 686.
30. H.I. West Jr, R.G. Lanier, M.G. Mustafa. $\text{Cr}^{52}(\text{p}, \text{n})^{52}\text{Mn}^{\text{g,m}}$ and $\text{Cr}^{52}(\text{d}, 2\text{n})^{52}\text{Mn}^{\text{g,m}}$ excitation functions. *Phys. Rev. C* 35(6) (1987) 2067.
31. A. Hermanne et al. Cross sections of deuteron induced reactions on $^{\text{nat}}\text{Cr}$ up to 50 MeV: Experiments and comparison with theoretical codes. *Nucl. Instr. Meth. B* 269(21) (2011) 2563.
32. A.A. Alharbi. Experimental Results Evaluation and Theoretical Study for the Production of the Radio Isotope ^{52}Mn Using P, D and A-Projectiles on V and Cr Targets. *Arab Journal of Nuclear Sciences and Applications* 49(3) (2016) 216.

33. E. Šimečková et al. Consistent account of deuteron-induced reactions on ^{nat}Cr up to 60 MeV. *Phys. Rev. C* 98(3) (2018) 034606.
34. R.B. Firestone, C.M. Baglin, S.Y. Frank Chu. *Table of Isotopes: 1999 Update*. 8th Edition. 224 p.
35. P.P. Coetzee, M.A. Peisach. Activation cross sections for deuteron-induced reactions on some elements of the first transition series, up to 5.5 MeV. *Radiochimica Acta* 17(1) (1972) 1.
36. A.T.J. Klein, F. Rösch, S.M. Qaim. Investigation of $^{50}\text{Cr}(d, n)^{51}\text{Mn}$ and $^{nat}\text{Cr}(p, x)^{51}\text{Mn}$ processes with respect to the production of the positron emitter ^{51}Mn . *Radiochimica Acta* 88(5) (2000) 253.
37. N. Baron, B.L. Cohen. Activation cross-section survey of deuteron-induced reactions. *Phys. Rev.* 129(6) (1963) 2636.

Глара Фуад Хасан^{1,2,3,*}, Едріс Мухаммад-Тохір Нурі¹, Флавія Гроппі^{2,3}

¹ Фізичний факультет, Педагогічний коледж, Університет Салахаддіна, Ербіль, Ірак

² Фізичний факультет, Міланський університет, Мілан, Італія

³ Лабораторія прискорювачів та прикладної надпровідності (LASA), Фізичний факультет, Міланський університет і Національний інститут ядерної фізики (INFN), Сеграте, Італія

*Відповідальний автор: gelara.hassan@su.edu.krd

ОЦІНКА ПЕРЕРЕЗІВ ДЛЯ РАДІОНУКЛІДІВ, ЩО ВИКОРИСТОВУЮТЬСЯ В ПОЗИТРОННО-ЕМІСІЙНІЙ ТОМОГРАФІЇ, З ВИКОРИСТАННЯМ КОДУ EMPIRE 3.2.2 З РІЗНИМИ МОДЕЛЯМИ ЩІЛЬНОСТЕЙ ЯДЕРНИХ РІВНІВ

Представлено результати розрахунків поперечних перерізів для ядерних реакцій на природному хромі (^{nat}Cr) для деяких радіонуклідів, що використовуються в позитронно-емісійній томографії: $^{nat}\text{Cr}(d, x)^{52g, m+}\text{Mn}$, $^{nat}\text{Cr}(d, x)^{54}\text{Mn}$, $^{nat}\text{Cr}(d, x)^{51}\text{Cr}$ та $^{nat}\text{Cr}(d, x)^{48}\text{V}$ з використанням статистичної ядерної програми EMPIRE 3.2.2 з різними моделями щільності ядерних рівнів. Результати порівняно з експериментальними даними, знайденими в літературі, і даними з різних електронних бібліотек TENDL.

Ключові слова: радіоізотопи Mn, позитронно-емісійна томографія, поперечні перерізи реакцій, ядерна медицина, код EMPIRE 3.2.2.

Надійшла/Received 07.10.2021

Evaluation of Atomic Recoil Spectra for Studies of Degradation in Semiconductor Devices

Brian D. Hehr¹

¹*Sandia National Laboratories, Albuquerque, NM, USA*

The evaluation of atomic recoil spectra from incident particle interactions underlies computational studies of neutron-induced damage in materials. For neutrons, typical impinging energies range from fractions of an eV (as from a room-temperature Maxwellian distribution) up to hundreds of MeV from cosmic ray-generated neutrons within Earth's atmosphere. Fission and fusion spectrum neutrons are also of interest in commercial and experimental applications where semiconductor materials (in discrete devices, circuits, sensors, etc.) are in sufficiently close proximity to the neutron source.

As neutron energy increases, additional nuclear reaction channels become accessible as respective threshold energies are exceeded. Nuclear reaction modelling codes like EMPIRE [1] and TALYS [2] are useful in characterizing recoil spectra from the various possible reactions. Broadly, as the transition is made from fission spectrum energies to D-T fusion (~14 MeV) energies, the recoil spectrum peak attributable mainly to elastic scattering splits into two distinct peaks—one at lower energy from elastic scattering, and one at higher energy from non-elastic interactions. The implications of these evaluations, including the impact of secondary charged-particle ejecta, will be discussed, and the application of TALYS to evaluation of recoil spectra will be addressed.

[1] M. Herman et al., *Nucl. Data Sheets*, **108**, 2655 (2007).

[2] A. J. Koning and D. Rochman, *Nucl. Data Sheets*, **113**, 2841 (2012).

Sandia National Laboratories is a multimission laboratory managed and operated by National Technology & Engineering Solutions of Sandia, LLC, a wholly owned subsidiary of Honeywell International Inc., for the U.S. Department of Energy's National Nuclear Security Administration under contract DE-NA0003525.

1 **The use of TENDL global parameters and TALYS calculations for**
2 **medical isotope production**

3 **M. Hussain^{1,2,†}**

4 ¹Institut für Neurowissenschaften und Medizin, INM-5: Nuklearchemie, Forschungszentrum
5 Jülich (FZJ), Jülich, Germany

6 ²Department of Physics, Government College University Lahore (GCUL), Lahore, Pakistan

7

8 * **Correspondence:**

9 Dr. Mazhar Hussain

10 dr.mazharhussain@gcu.edu.pk

11 **Abstract**

12 TALYS code has gained considerable attention for the calculations of nuclear reactions and
13 associated transport phenomenon. This user friendly and highly efficient code has replaced the
14 previously existing statistical and precompound model codes. It has been frequently used by the
15 community of medical radionuclide production. IAEA has also used its library to establish its
16 database for medical radionuclides. In most of the cases, the global optical models are
17 reproducing the experimental data very well but in some cases the TENDL database has large
18 deviations. To look into the problem, an example of a copper radionuclide is presented here. The
19 focus is on the production cross sections of Cu-67 that is a β^- -emitting radionuclide with a half
20 life of 61.9 h. It is suitable for targeted therapy. The calculations of production cross sections via
21 $^{68}\text{Zn}(p,2p)^{67}\text{Cu}$ reaction has been carried out. A comparison of the calculations with the
22 experimental data and with the TENDL library is presented.

23

Time-of-flight neutron elastic and inelastic cross section measurements of $^{206,208}\text{Pb}$ with the ELISA neutron spectrometer

J.K. Knijpstra

ESRIG, University of Groningen

Acquiring accurate nuclear cross section data is pertinent to the design of new Generation IV nuclear reactors, as uncertainties in cross section values are propagated in nuclear reactor models. Of particular importance are neutron scattering (elastic and inelastic) and (x,xn) reactions. These reactions contribute to the slowing down of the neutrons, modification of the neutron population, and the creation of new isotopes which can lead to radioprotection issues. Despite their importance, the cross sections of these interactions are experimentally poorly known. Therefore it is necessary to improve the precision of the existing nuclear data libraries. With this purpose, experiments are performed at the GELINA facility in Geel, Belgium, employing the time-of-flight (t.o.f.) method.

Priority goes to the measurement of the cross section measurements of the $^{206,208}\text{Pb}(n,n)$ and $^{206,208}\text{Pb}(n,n'\gamma)$ reactions. These cross section data are valuable for the lead-cooled fast reactors ALFRED. New measurements are required for a proper evaluation of the coolant density and the Doppler effects.

At GELINA, a pulsed white neutron beam is produced via photo-nuclear reactions induced by brehmstrahlung caused by LINAC electrons striking a uranium target. The neutrons travel towards a target along a long flight path, allowing their incident energies to be determined by measuring their t.o.f.. The ELISA [1] (Elastic and Inelastic Scattering Array) neutron spectrometer at GELINA consists of 32 liquid organic scintillation detectors, designed to measure differential elastic and inelastic cross-sections. This setup is planned to be extended with a number of NaI(Tl) detectors, allowing for neutron-gamma coincidence measurements to be performed and therefore for more precise inelastic cross section determination.

[1] M. Nyman et al., EPJ Web of Conferences 239, 17003 (2020).

Development of a detection technique of nuclear fuel materials using photonuclear reactions

R. Kunitomo¹, T. Katabuchi¹, C. Ishizuka¹, and H. Sagara¹

¹Tokyo Institute of Technology

Nuclear security at nuclear reactor facilities is a significant concern, particularly with regards to the theft and smuggling of nuclear material, as well as sabotage of the facilities. One crucial task to prevent these security incidents is the development of non-destructive detection techniques for identifying nuclear material. Although numerous techniques have been proposed, further study is still required to meet the necessary requirements.

In this research, a new non-destructive technique is being developed to detect nuclear material. High-energy gamma-rays are employed as probes for this purpose. When a high-energy photon interacts with nuclear material, such as uranium or plutonium, it induces nuclear fission and emits fast neutrons. These neutrons can be detected using neutron detectors such as liquid scintillator. Neutrons possess a high power of penetrability, enabling the detection of nuclear material even if it is concealed within a container made of high-Z materials [1].

The feasibility of this technique will be evaluated through simulations and experiments using an accelerator.

[1] R. Kimura, et al., J. Nucl. Sci. Technol. 53, 1978 (2016).

Neutron inelastic scattering cross section measurements at Lawrence Berkeley National Laboratory

T.A. Laplace¹, B.L. Goldblum^{1,2}, J.A. Brown¹, L.A. Bernstein^{1,2}, J.C. Batchelder¹, D.L. Bleuel³, C.A. Brand^{1,3}, A. Georgiadou¹, J.M. Gordon¹, J.J. Manfredi⁴, K. Myers¹, T.S. Nagel¹

¹ *University of California, Berkeley*

² *Lawrence Berkeley National Laboratory*

³ *Lawrence Livermore National Laboratory*

⁴ *Air Force Institute of Technology*

Neutron inelastic scattering cross section data are key inputs for basic science studies and the modeling of various applications, including radiation shielding, nuclear energy, stockpile stewardship, and proliferation detection. The need for new data was identified in recent work [1, 2]. The Gamma-Energy Neutron-Energy Spectrometer for Inelastic Scattering (GENESIS) has been assembled and commissioned at the Lawrence Berkeley National Laboratory 88-Inch Cyclotron to measure inelastic scattering cross sections in the ~ 1 –20 MeV neutron energy range. The detector array is composed of 26 2-inch right cylinders of EJ-309 pulse-shape discrimination capable organic liquid scintillators, three 4-crystal segmented high-purity germanium (HPGe) Eurisys Clover detectors with BGO anti-Compton shields [3], and a LaBr₃ inorganic scintillator. Neutrons are produced by impinging a deuteron beam accelerated by the cyclotron onto a thick target (carbon or beryllium) in the cyclotron vault producing an intense, broad spectrum neutron beam which is collimated into a ~ 10 -cm-diameter beam on a thin target (~ 10 –40 g) made of the isotope of interest positioned approximately 7 meters downstream from the neutron production target. The neutron energy distribution is tunable by selection of the deuteron energy between 14 and 50 MeV. Signals from γ -rays and neutrons detectors were read out using four time-synced 16-channel MDPP-16 digital pulse processing modules. The array was characterized using a 0.5 mCi ²⁵²Cf source in conjunction with Geant4 modeling. In-beam data were taken on several materials of interest including ⁵⁶Fe, ²³⁸U, ³⁵Cl, ²³Na, and ¹²C. A forward modeling approach to data analysis is currently under development, coupling high-fidelity Geant4 simulations to TALYS generated cross sections and minimized against measured γ rays and neutron distributions.

- [1] L. Bernstein, C. Romano, D. Brown, R. Casperson, M-A. Descalle, M. Devlin, C. Pickett, B. Rearden, C. Vermeulen, Final Report for the Workshop for Applied Nuclear Data Activities (WANDA), White paper LLNL Report LLNL-PROC-769849 (2019).
- [2] S. McConchie, et al., Report No. ORNL/TM-2021/1900, (2021).
- [3] G. Duchene, F.A. Beck, P.J. Twin, G. de France, D. Curien, L. Han, C.W. Beausang, M.A. Bentley, P.J. Nolan, J. Simpson, Nucl. Instrum. Meth. Phys. Res. A **432**, (1999).

^{47}Sc production for medical applications: cross-section optimization based on genetic algorithm

Yuliia Lashko^{1,2}, Francesca Barbaro^{1,3}, Luciano Canton¹, and Lisa Zangrando¹

¹ *National Institute for Nuclear Physics, Padova Division, Padova, Italy*

² *Bogolyubov Institute for Theoretical Physics, Kyiv, Ukraine*

³ *Pavia University, Physics Department, Pavia, Italy*

^{47}Sc is a promising radionuclide for the realization of new radiopharmaceuticals suitable both for therapy and diagnostic purposes [1]. It can be produced by irradiating an enriched titanium target (composed of $^{48-50}\text{Ti}$) with a proton beam. In this report, we consider $^{49}\text{Ti}(p,x)$ reactions. It is crucial to evaluate accurately cross sections of ^{47}Sc production, as well as for contaminants $^{43,44,46,48}\text{Sc}$, and for other radionuclides, such as $^{42,43}\text{K}$ and ^{48}V , where nuclear data exist. A precise description of the cross sections allows calculation of production yields and selection of the possible energy ranges suitable for producing ^{47}Sc with sufficient purity for medical applications. To date, no measurements of $^{49}\text{Ti}(p,n2p)^{47}\text{Sc}$ have been published yet and the first preliminary experimental data for this reaction have been produced at ARRONAX by the LNL-REMIX collaboration [2].

For the evaluation of the cross sections we have used TALYS code, which is a computer program for the analysis and prediction of nuclear reactions involving p, d, t, $^3,^4\text{He}$ beams in the eV - 200 MeV energy range and for target nuclides of mass 12 and heavier [3]. For predicting cross sections, tabulated nuclear-level densities derived from Hartree-Fock microscopic models are used at excitation energies where discrete-level information is not available or incomplete. Furthermore, these calculated microscopical level densities can be adjusted in TALYS code to experimental data via a scaling function containing two adjustment parameters. For our purpose, we considered 6 pairs of the parameters describing the level densities of 6 compound nuclei ($^{43,44}\text{Sc}$, $^{46,47,48}\text{Sc}$, ^{48}V). The optimization of these parameters to fit the above-mentioned cross sections is a challenging problem. A genetic algorithm (GA), which is a random-based evolutionary algorithm inspired by Darwin's theory of natural selection [4], is an efficient tool for this goal.

We have applied genetic algorithm to optimize the large set of measured cross sections relevant for ^{47}Sc production from ^{49}Ti target. It is found that GA represents an efficient optimization tool to provide a more accurate description of the cross sections. However, the improvement in the description of cross sections is in some cases obtained at the expense of the phenomenological reproduction of the cumulative number of levels. We are presently investigating how to adapt the GA approach to obtain a good reproduction of cross sections without spoiling the description of the nuclear-level cumulatives.

- [1] K. Domnanich et al., EJNMMI radiopharm. chem. **2**, 5 (2017).
- [2] L. De Dominicis, L. Mou, G. Pupillo, private communication
- [3] S. Goriely et al., Astron. Astrophys., **487**, 767 (2008).
- [4] S. Luke, Essentials of Metaheuristics (Lulu publisher) (2013).

Device and method for low-uncertainty and high-efficiency neutron time-of-flight spectrometry

Jorge Martín-Yi¹, Daniel López-Aldama¹, Guido Martín-Hernández¹, Pierfrancesco Mastinu², Elizabeth Musacchio González²

¹ *Centro de Aplicaciones Tecnológicas y Desarrollo Nuclear, 30 No. 502 Playa, La Habana, Cuba*

² *INFN – Laboratori Nazionali di Legnaro, Viale dell'Università 2, 35020 Legnaro, Italy*

In neutron spectrometry, a paramount magnitude to obtain the neutron energy spectrum is the detection efficiency as a function of the neutron energy. By Monte Carlo simulation of the detector, the efficiency is calculated. However, the systematic uncertainty in this calculation are poorly estimated. In the current work, a boron-based neutron detection system has been used to measure, by time-of-flight, neutron fields produced by the ${}^7\text{Li}(p,n){}^7\text{Be}$ reaction. The detection system is based on a neutron-to-gamma converter attached to a gamma detector where the converter is a highly enriched (>99%) ${}^{10}\text{B}$ disk [1]. Eventually, a neutron reacts with a ${}^{10}\text{B}$ nucleus forming the excited ${}^{11}\text{B}^*$ nucleus that splits into ${}^4\text{He}$ and ${}^7\text{Li}$ nuclei. The latter nucleus is produced approximately 94 % of the time in its excited state, decaying by the prompt emission of a 478 keV γ ray. This photon is detected in a $\text{Bi}_4\text{Ge}_3\text{O}_{12}$ scintillation crystal. Li-glass scintillators are some of the most used neutron detectors based on the ${}^6\text{Li}(n,\alpha){}^3\text{H}$ reaction. Therefore, we compare this detector with our ${}^{10}\text{B}$ - $\text{Bi}_4\text{Ge}_3\text{O}_{12}$ arrangement in terms of absolute detection efficiency and efficiency uncertainty. Propagating the uncertainties available in the evaluated nuclear data file, the uncertainties of these efficiencies were estimated. To perform these analyses, random libraries based on covariance files from ENDF/B-VIII.0 [2] and TENDL-2021 [3], for each detector with the help of the NJOY [4] and SANDY [5] codes were obtained. Due to the superior number of isotopes, with larger uncertainties in the cross section data, present in the Li-glass detector compared to the boron-based detector, smaller uncertainties were yielded for the last one. For our detector, at 30 keV of neutron energy, about three times higher counting efficiency was observed, compared to a commercially available Li-glass scintillator.

[1] G. Martín-Hernández, *Phys. Rev. C* **94**, 034620 (2016)

[2] D.A. Brown *et al.*, *Nuclear Data Sheets*, Vol. **148**, 1 (2018)

[3] A.J. Koning *et al.*, *Nuclear Data Sheets*, Vol. **155**, 1 (2019)

[4] R.E. MacFarlane, A.C. Kahler, *Nuclear Data Sheets*, Vol. **111**, 2739 (2010)

[5] L. Fiorito *et al.*, *Annals of Nuclear Energy*, Vol. **101**, 359 (2017)

A Mirror $1/2^+$ states of ${}^9\text{Be}$ and ${}^9\text{B}$ in the complex scaling method

M. Odsuren

School of Engineering and Applied Sciences and Nuclear Research Center, National University of Mongolia, Ulaanbaatar 210646, Mongolia

Studies of mirror nuclei are important in understanding of the nuclear structure. However, in spite of considerable experimental [1, 2] and theoretical [3] efforts, the location of the first excited state of the ${}^9\text{B}$ nuclei has not yet determined and the structures of the first excited $1/2^+$ states in mirror nuclei ${}^9\text{Be}$ and ${}^9\text{B}$ are still an open problem. The nuclei ${}^9\text{Be}$ and ${}^9\text{B}$ are considered to have an $\alpha + \alpha + N$ (N =neutron or proton) structure according to the lowest three-body thresholds, and to be the Borromean systems. Except for the ground state $3/2^-$ of ${}^9\text{Be}$, all states including the ground state of ${}^9\text{B}$ are unbound. Therefore, in order to study the first excited states of ${}^9\text{Be}$ and ${}^9\text{B}$, it is necessary to calculate the $\alpha + \alpha + N$ three-cluster systems under a correct boundary condition for unbound states.

We investigated the structure of the first unbound state of ${}^9\text{Be}$ located just above the $\alpha + \alpha + n$ threshold energy applying the $\alpha + \alpha + n$ three-body model [3] and the complex scaling method (CSM) [4]. In the results, we found that the ${}^9\text{Be}(1/2^+)$ state has a virtual-state character of an s -wave neutron around the ${}^8\text{Be}(0^+)$ cluster.

We study the existence and structure of the ${}^9\text{B}(1/2^+)$ state based on our previous method for the $\alpha + \alpha + N$ cluster model with the complex scaling method that well explains the measured photo-disintegration cross section for the ${}^9\text{Be}(1/2^+)$. We find two resonances at the energies of $E_1^{res} = 1.81$ MeV with a decay width $\Gamma = 1.98$ MeV and $E_2^{res} = 2.38$ MeV, $\Gamma = 1.81$ MeV in ${}^9\text{B}$. The charge radii and the three-body channel configurations are calculated to see the properties of two resonances. We also calculate the level density of two resonances, which indicates the difficulty to distinguish them in the energy distribution.

- [1] Akimune, H., Fujimura, M., Fujiwara, M., Hara, K., Ihikawa, T., Utsunomiya, H., Yamagata, T., Yamasaki, K., Yosoi, M., Phys. Rev. C **64**, 041305 (2001).
- [2] Tiede, M.A., Kemper, K.W., Fletcher, N.R., Robson, D., Caussyn, D.D., Bennett, S.J., Brown, J.D., Carford, W.N., Jones, C.D., Watson, D.L., Rae, W.D.M., Phys. Rev. C **52**, 1315 (1995).
- [3] Odsuren, M., Kikuchi, K., Myo, T., Aikawa M., Katō, K., Phys. Rev. C **92**, 014322 (2015).
- [4] Ho, K., Phys. Rep. **99**, 1 (1983).

Thermal neutron capture cross-section and resonance integral measurements of $^{186}\text{W}(n,\gamma)^{187}\text{W}$ reaction using the thermal column neutron source at the Dalat research reactor

Bich Thuy Nguyen¹, Thi Tu Anh Trinh², Ngoc Son Pham¹, Dong Vu Cao¹

¹ *Dalat University, 01 Phu Dong Thien Vuong Str., Dalat, Vietnam*

² *Dalat Nuclear Research Institute, 01 Nguyen Tu Luc Str., Dalat, Vietnam*

The thermal neutron radiative capture cross-section (σ_0) and the resonance integral (I_0) of the reaction $^{186}\text{W}(n,\gamma)^{187}\text{W}$ were measured by the thin foil activation method using the well thermalized neutron source at the graphite thermal column facility of the Dalat research reactor. The activities of the irradiated foil samples were measured using a high resolution HPGe gamma-ray spectrometer. The recent updated values of gamma-rays intensities and decay half-life of the ^{187}W nucleus were applied in this experiment for a significant improve of the cross section results in comparison with the previous measurements. The thermal neutron captures cross section and the resonance integral of the $^{186}\text{W}(n,\gamma)^{187}\text{W}$ reaction were determined relative to the standard reaction $^{197}\text{Au}(n,\gamma)^{198}\text{Au}$. The obtained results are 31.76 ± 0.63 and 429.2 ± 25.6 barns for σ_0 and I_0 respectively. The comparison and discussions of the discrepancies between our results and previous measured values were summarized.

Keywords: Thermal neutron, epithermal neutron, cross-section, resonance integral.

Cross section uncertainties and their impact on background studies

M. Pârnu¹, P. Krawczun², V. A. Kudryavtsev²

¹ Faculty of Physics, University of Bucharest, POBox MG-11 Bucharest-Magurele, Romania

²Department of Physics and Astronomy, University of Sheffield, Sheffield S3 7RH, UK

In rare events physics experiments an important step is to understand the radiological and cosmogenic backgrounds. The sources of background that can impact the sensitivity and results of the low event rate experiments include neutrons generated from (α , n) reactions and spontaneous fission from U and Th decay chains. In particular, neutrons represent an important background for dark matter and proton decay searches, neutrinoless double beta decay, low-energy neutrino physics such as solar and supernova neutrinos, and reactor neutrino experiments.

Experimental data for (α ,n) cross sections for the energy range of interest (less than 10 MeV) are scarce and sometimes not in agreement with each other. Hence, we need to use nuclear reaction codes (TALYS [1, 2] and EMPIRE [3]) along with evaluated data such as ENDF [4], TENDL and JENDL [5].

Both TALYS and EMPIRE are statistical model codes, and thus may not be able to reliably calculate (α ,n) cross-sections. These codes cannot properly model the resonance region of the cross-sections. Hence, for low-A nuclei experimental data should be used. However, for medium and high mass numbers we need to rely on calculations because the data are scarce or unavailable. For low-mass nuclei, by incorporating experimental measurements and theoretical calculations, JENDL-2005 database provides reliable data for (α ,n) reactions, including the resonance region.

In this work, the cross-sections of (α ,n) reactions for a number of materials are calculated with TALYS 1.96 and EMPIRE 3.2.3 considering different optical model parameters and are compared with the experimental data where available. Branching ratios for transitions to excited states have been calculated as well. The input cross-sections in SOURCES4 [6, 7] library have been optimized by combining experimental data with calculated cross-sections where the data are unavailable or not fully reliable. Neutron yields and neutron spectra have been calculated using the SOURCES4 code.

These results as a function of the alpha energy are compared with the experimental ones from thick target neutron yields obtained with alpha beams. This procedure allows us to estimate the accuracy of our calculations of neutron background in various experiments.

[1] A. J. Koning, et al., Nuclear Data Sheets **155** (2019): 1-55.

[2] A.J. Koning and D. Rochman, Nuclear Data Sheets **113** (2012) 2841.

[3] M. Herman, et al., Nucl. Data Sheets, **108** (2007) 2655-2715.

[4] D. A. Brown, et al., Nucl. Data Sheets **148** (2018)1.

[5] T. Murata et al., JAEA-Research 2006-052

[6] W. B. Wilson, et al., Radiation Protection Dosimetry, **115** (2005) 117–121

[7] W. B. Wilson, et al., Technical Report LA–13639-MS (1999)

Nuclear data uncertainties and adjustments using deterministic and Monte-Carlo methods along with PWR measurements

V. Salino^{1,2}, D. Rochman³, E. Dumonteil², F. Malvagi² and A. Hébert¹

¹*École Polytechnique de Montréal, Institut de Génie Nucléaire*

P.O. Box 6079, Station Centre-Ville, Montréal, Qc., H3C 3A7, Canada

²*Institut de Radioprotection et Sûreté Nucléaire (IRSN), PSN-RES/SNC/LN*

BP 17, Fontenay-aux-Roses, 92262, France

³*Paul Scherrer Institut (PSI), Laboratory for Reactor Physics and Thermal-Hydraulics (LRT)
Forschungsstrasse 111, 5232 Villigen, Switzerland*

Nuclear power plants safety relies partly on predictions from numerical simulations. Their uncertainties must therefore be evaluated. In PWR reactor physics, the simulations' uncertainties are nowadays estimated on the basis of the differences between existing measurements and the corresponding simulations. This approach leads to weaknesses in the estimation of uncertainties. For example, an unprecedented situation (possibly accidental) can induce more deviations than those seen in the past. Moreover, these uncertainties are often based on differences between measurements and *adjusted* simulations, i.e. carried out *after* the measurements and by *forcing* the simulations as close as possible to the measurements. The residual deviation thus leads to consider compressed uncertainties. This method of evaluating uncertainties can therefore be improved. To further increase robustness, the proposed approach is to return to the fundamentals : the sources of errors in the simulations. The two main types discussed here are the following. On the one hand, physical and numerical approximations introduce deterministic biases, which can be evaluated as the difference with Monte-Carlo. On the other hand, the nuclear data uncertainties, that arise from the limited human understanding of nuclear physics, have been propagated with a Total Monte-Carlo approach through standard deterministic methods, affected by deterministic biases, and with Monte-Carlo transport. Comparison of the two led to this central finding : for variations in nuclear data typically corresponding to their uncertainties, the deterministic biases can be considered identical between different samples [1]. Although seemingly insignificant, this excellent agreement opens new perspectives. Indeed, the different samples of nuclear data can be propagated with deterministic methods, and then corrected at once with a single Monte-Carlo reference solution. This dual approach benefits from the best of both deterministic and Monte-Carlo worlds. Beyond this first topic about the propagation of uncertainties, a second topic – closely related – is covered : adjustments to measurements. It is legitimate to consider that simulations should reproduce measurements performed experimentally on real PWR reactors. However, the most common adjustment methods are based on non-universal error compensations, which affects their extrapolation capabilities. Moreover, the question of uncertainties is absent in these adjustments. These two issues are addressed with nuclear data uncertainty propagation, elimination of the deterministic bias (as seen above) and the BFMC method. Among the plausible nuclear data, those in better agreement with experimental measurements are considered most likely. The nuclear data uncertainties are reduced in a balanced way, without showing signs of overfitting [1]. By mobilizing a physical and universal knowledge of the root causes of errors (nuclear data, deterministic bias), the exploited methods present strong arguments, that can claim a better extrapolation capability than standard methods of uncertainty evaluation and adjustment, thus improving nuclear power plants safety.

- [1] V. Salino, D. Rochman, E. Dumonteil, F. Malvagi, A. Hébert, *Nuclear data uncertainties and adjustments using deterministic and Monte-Carlo methods along with PWR measurements*, International Conference on Mathematics & Computational Methods Applied to Nuclear Science & Engineering (M&C), Niagara Falls, Canada (2023). <https://hal.science/irs-n-04095487v1>

Analysis of $^{209}\text{Bi}(\gamma, xn)$ nuclear reactions

Rade Smolović¹, Nikola Jovančević¹, Miodrag Krmar¹ and David Knežević²

¹Faculty of Science, University of Novi Sad, Novi Sad, Serbia

²Institute of Physics Belgrade, Belgrade, Serbia

In this paper, the cross section values for the $^{209}\text{Bi}(\gamma, xn)$ nuclear reactions were calculated using the different models for the level density and the radiation strength function by the TALYS code [1]. Based on the obtained data, the yields of nuclear reactions were determined. The results of this theoretical calculation were compared with experimental data in the range up to 100 MeV [2].

[1] A.J. Koning and D. Rochman, "Modern Nuclear Data Evaluation With The TALYS Code System", Nuclear Data Sheets 113 (2012) 2841.

[2] Demichev, M., Abou El Azm, S., et al A.Study of $^{209}\text{Bi}(\gamma, xn)$ Reactions in Energy Region up To 100 MeV, Physics of Atomic Nuclei, 85(6), pp. 805–812, 2022.

The theoretical estimation of a combined production of ^{68}Ga and ^{32}P radioisotopes were investigated using a medical cyclotron. Protons are used in the $^{68}\text{Zn}(p,n)$ reaction to produce the medical isotope ^{68}Ga . The neutrons from the $^{68}\text{Zn}(p,n)^{68}\text{Ga}$ reaction are used to launch the $^{32}\text{S}(n,p)$ reaction to produce ^{32}P radioisotope. The cross section of these reactions was calculated using TALYS 1.9 code and compared with the available experimental results. SRIM-2013 code was used to calculate the stopping power and range of protons in the ^{68}Zn target and GEANT4 toolkit was used to evaluate the proton and neutron flux within the ^{68}Zn and ^{32}S targets, respectively. The theoretical and simulation production yield of ^{68}Ga and simulation production yield of ^{32}P radioisotopes in each reaction were calculated. The results show that the Monte Carlo method can be used for the design and optimization the targets and calculation of production yield for ^{68}Ga and ^{32}P radioisotopes.

Cross-sections of photonuclear reactions ${}^{\text{nat}}\text{Ni}(\gamma, \text{pxn})^{55-58}\text{Co}$: experimental and calculated in the TALYS code

**I.S. Timchenko^{1,2}, O.S. Deiev², S.N. Olejnik², S.M. Potin²,
V.A. Kushnir², V.V. Mytrochenko^{2,3}, S.A. Perezhogin² and A. Herzán¹**

¹ Institute of Physics, Slovak Academy of Sciences, SK-84511 Bratislava, Slovakia

² NSC "Kharkov Institute of Physics and Technology", National Academy of Sciences of Ukraine, 1 Academichna Str., Kharkiv, 61108, Ukraine

³ CNRS/IJCLAB, 15 Rue Georges Clemenceau Str., Orsay, 91400, France

A sufficient dataset exists on experimental cross-sections in the GDR energy region. In the case of one- or two-particle reactions, different theoretical concepts give rather similar predictions. Differences between various theoretical models become more noticeable for reaction cross-sections with three or more particles in the reaction channel. Experimental data for multiparticle reactions in a wide range of atomic masses A and beam energies E are therefore very important as they provide a test ground for theoretical models.

Our research presented here focuses on the study of multiparticle photonuclear reactions on nickel, which is an important structural and surface coating material, used in accelerator nuclear technology and accelerator-driven sub-critical systems. The experiment was performed using the beam from the NSC KIPT electron linear accelerator LUE-40. The parameters of the accelerator complex are given in [1]. To obtain values of flux-averaged cross-sections $\langle\sigma(E_{\gamma\text{max}})\rangle$ the γ -activation and off-line γ -ray spectrometry were used. The total cross-sections $\langle\sigma(E_{\gamma\text{max}})\rangle$ for the photonuclear reactions ${}^{\text{nat}}\text{Ni}(\gamma, \text{pxn})^{55-58}\text{Co}$ have been measured in the range of end-point energies of bremsstrahlung spectrum $E_{\gamma\text{max}} = 35\text{--}94$ MeV. The modeling of bremsstrahlung flux that impinged on target was performed using the GEANT4.9.2 [2] simulation toolkit with taking into account the actual geometry of the experiment and the energy distribution in the electron beam and additionally monitored by the yield of the ${}^{100}\text{Mo}(\gamma, n){}^{99}\text{Mo}$ reaction.

The obtained values of $\langle\sigma(E_{\gamma\text{max}})\rangle$ for the production of ${}^{55,56,57}\text{Co}$ isotopes in the ${}^{\text{nat}}\text{Ni}(\gamma, \text{pxn})$ reactions are in good agreement with data from [3]. For the ${}^{\text{nat}}\text{Ni}(\gamma, \text{pxn})^{58}\text{Co}$ reaction, our measured cross-section value is higher than the cross-section from [3] but agrees with data adopted from [4].

The theoretical values of $\langle\sigma(E_{\gamma\text{max}})\rangle_{\text{th}}$ were calculated using the cross-sections $\sigma(E)$ from the TALYS1.95-1.96 code [5]. The cross-section calculations in the TALYS1.95 and TALYS1.96 codes (TENDL-2019 and TENDL-2021) differ by more than a factor of 2 for the photonuclear reaction ${}^{\text{nat}}\text{Ni}(\gamma, \text{pxn})^{58}\text{Co}$. The obtained experimental $\langle\sigma(E_{\gamma\text{max}})\rangle$ values are in a good agreement with theoretical predictions based on the TALYS1.96 code. The contributions of dominant reactions on natural Ni to the production of ${}^{55-58}\text{Co}$ nuclei were estimated based on the theoretical prediction from the TALYS1.96 code.

[1] M.I. Aizatskiy, V.I. Beloglazov, V.N. Boriskin, et al., *Probl. Atom. Sci. Tech.* **3**, 60 (2014).

[2] S. Agostinelli, J.R. Allison, K. Amako, et al., *Nucl. Instrum. Meth. Phys. Research.* **A506**, 250 (2003).

[3] H. Naik, G. Kim, Th.H. Nguyen, et al., *J. Radioanal. Nucl. Chem.* **324**, 837 (2020).

[4] A.G. Kazakov, Ju.S. Babenya, T.Y. Ekatoeva, et al., *Molecules* **27**, 1524 (2022).

[5] A.J. Koning and D. Rochman, *Nuclear Data Sheets* **113**, 2841 (2012).

Statistical Model Calculations with TALYS for Sn Isotopes

M.Twisha^{1,2,*}, A.Gupta^{1,2}, S.Bhattacharjee^{1,2}, and A.Mukherjee^{1,2}

¹*Nuclear Physics Division, Saha Institute of Nuclear Physics, Kolkata - 700064, INDIA and*

²*Homi Bhabha National Institute, Mumbai,INDIA*

Introduction

Putting a strong stamp on the origin of p -nuclei is an open challenge in nuclear astrophysics. The p -process or photodisintegration being a very important mechanism for production of these proton rich nuclei, the γ - process reaction rates are derived from proton capture reaction rates via reciprocity theorem. Nuclear reaction rates are essential ingredients for investigation of energy generation and nucleosynthesis processes in stars. These reaction rates are functions of the densities of the interacting nuclei, their relative velocities and reaction cross-sections. To estimate the abundance of any element, reaction rates of all the reactions involved in the synthesis of that element needs to be known and it is given by product of reaction cross section and velocity distribution of projectiles. The stellar temperatures are of the order of GK which translates to lower energies where charge particle induced reactions are suppressed due to coulomb barrier. Since the reaction network for p -process is vast and the cross sections are low, scarcity of experimental data at the astrophysically relevant energies calls for theoretical models to predict the cross section and estimate the reaction rates of unmeasured reactions. Generally experimental cross sections are larger than the statistical model predictions which underestimates the reaction rates at low energies, So, measurement of cross section at low energies and new statistical model calculations are highly desirable.

The success of a statistical model depends on the various nuclear models taken as input. To predict the reliability of predictions of these models, we compare the experimental data with calculated cross sections. one such approach is TALYS which employs Hauser Feshbach Statistical model.

TALYS Calculation

Most of the reactions in stars proceeds through the formation of a Compound Nucleus (CN) for which Neils Bohr hypothesized that decay of a CN is independent of its mode of formation. Hauser Feshbach statistical model calculates cross sections for such CN states taking care of angular momentum correlations in the entrance and exit channels. The nuclear inputs that goes in the calculation are masses, nuclear level density (NLD), optical model potentials (OMP) and gamma strength function (γ SF). Hauser Feshbach cross section is given by

$$\sigma \propto \tau_i \tau_o / \tau_{tot}$$

where, τ is the transmission probability and i, o label entrance and exit channels, respectively.

The cross sections for the proton capture reactions with $^{112,114}\text{Sn}$ have already been measured in the energy region relevant to p -process and compared with theory. To check for a better agreement of experimental data of Sn-isotopes with theory, in this work, theoretical analysis have been performed for Sn-isotopes, ^{112}Sn and ^{114}Sn using TALYS whose experimental data is available in literature[1, 2]. The effect of different models of NLD, OMP and γ SF were investigated by alternately varying one and keeping other two fixed at defaults. It was observed that in the energy domain of the present study, the σ_{HF} is insensitive to different models of γ SF and NLD but

*Electronic address: twisha.munmun@saha.ac.in

Isotope	E_{lab} (MeV)	V_0 (MeV)	r_v (fm)	a_V (fm)	W_0 (MeV)	r_w (fm)	a_w (fm)
^{112}Sn	27.45	51.92	1.17	0.75	7.50	1.32	0.51
	27.45	47.07	1.26	0.65	9.58	1.16	0.68
	16	55.46	1.2	0.7	10.38	1.25	0.65
^{114}Sn	22	50.0	1.25	0.65	10.0	1.30	0.6

TABLE I: Optical potential parameters adjusted to proton elastic scattering on ^{112}Sn and ^{114}Sn at different lab energies.

it does depend on various models of OMP.

Optical potentials describe interaction between target and incoming projectile. The phenomenological optical potential employed in TALYS is given as

$$\begin{aligned}
 U = & -V_v(E)f(r) - iW_v(E)f(r) \\
 & - 4ia_wW_D(E)g(r) \\
 & + V_{SO}(r,E)(l.s) + V_C(r)
 \end{aligned}$$

where, $f(r)$ is woods saxon form function and $g(r)=df(r)/dr$. The normalisation parameters were adjusted to acquire the elastic scattering optical model parameters in order to describe the experimental data extracted from ref [1, 2].

The sets of optical model parameters adjusted with elastic scattering of proton on ^{112}Sn [3, 4] and ^{114}Sn [5] used in this analysis are given in table I

Summary

Hauser Feshbach statistical model calculations were performed to describe the experimental cross sections of $^{112}\text{Sn}(p,\gamma)^{113}\text{Sb}$ and $^{114}\text{Sn}(p,\gamma)^{115}\text{Sb}$ [1, 2] using TALYS. On investigation, σ_{HF} turns out to be insensitive to different models for NLD and γSF in the energy domain of the present study, namely 2-9 MeV for both the reactions but depends on OMP parameters. Several OMP parameter sets optimized with proton elastic scattering data [3-5] were used to calculate cross sections. S-Factor was then plotted against proton lab energy and compared with literature data, Fig.1 and Fig.2.

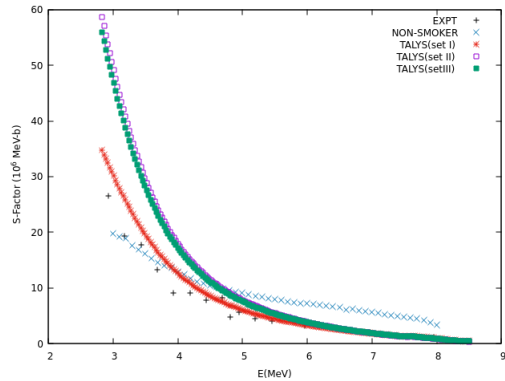


FIG. 1: S-factors for the $^{112}\text{Sn}(p,\gamma)^{113}\text{Sb}$ reaction as a function of proton energy(lab) compared with the experimental data and theoretical results from the NON-SMOKER code from [1].

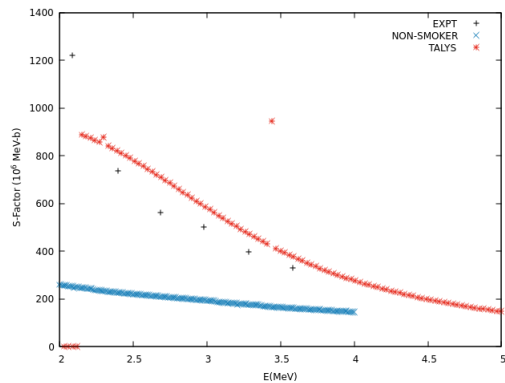


FIG. 2: Astrophysical S-factors for the $^{114}\text{Sn}(p,\gamma)^{115}\text{Sb}$ reaction. Also shown are the experimental data and predictions using the NON-SMOKER calculation from [2].

References

- [1] F.R. Chloupek et al., Nuclear Physics A652(1999) 391-405.
- [2] Michael A. Famiano et al., Nuclear Physics A802(2008) 26-44.
- [3] P.J.Biankert et al., Nuclear Physics A356(1981) 74-96.
- [4] G.S.Mani et al., Nuclear Physics A165(1971) 384-392.
- [5] P. Guazzoni et al., Physical Review C 85, 054609 (2012).

Effects of level density a-parameter in the framework of preequilibrium model for ^{58}Ni (n, xp) reaction at 8, 9, 9.4 and 11 MeV

L. Yettou¹, **M. Belgaid**¹, **N. Beloaudah**¹, **F. Kadem**¹, and **N. Amrani**²

¹ *University of Sciences and Technology Houari Boumediene, faculty of physics, Algiers
Algeria*

² *University Ferhat Abbas, Sétif, Algeria*

Nickel is a major component of austenitic steel that is widely employed in the nuclear industry and it is an important structural material for nuclear applications [1]. In this study, the calculations of proton emission spectra produced by ^{58}Ni (n, xp) reaction are used in the framework of preequilibrium model by using Talys code [2]. The main purpose of this work is to investigate the sensitivity of level density a-parameter in the framework of preequilibrium model. Exciton model [3] predictions were used, and some necessary parameters have been investigated for our calculations. The level density a-parameter affects strongly the fit for ^{58}Ni (n, xp) reaction and the comparison with experimental data [4] shows clear improvement over the exciton model [3] calculations.

[1] Dispersive coupled-channels optical model potential with soft-rotor couplings for Cr, Fe, and Ni isotopes. Rui Li et al, PHYSICAL REVIEW **C87**, 054611 (2013).

[2] A. KONING, S. HILAIRE and M. C. DUIJVESTIJN, "Talys-1.0," Proc. Int. Con. Nuclear Data for Science and Technology (ND-2007), Nice, France, April 22-27, 2007.

[3] J. J. Griffin, Phys. Rev. Lett., **17**, 478 (1996).

[4] Experimental Nuclear Reaction Data (EXFOR) Database Version of March 16, 2015, <https://www-nds.iaea.org/exfor/exfor.htm> (current as of July 12, 2015).